Expired Drug (pantoprazole sodium) as a Corrosion Inhibitor for High Carbon Steel in Hydrochloric Acid Solution

A.S. Fouda[1,], H.Ibrahim[2], S.Rashwaan[2], A. El-Hossiany[3], R.M. Ahmed[1]*

[1] Department of Chemistry, Faculty of Science, El-Mansoura University, El-Mansoura-35516, Egypt,
[2] Department of Chemistry, Faculty of Science, Suez Canal University. Ismailia, Egypt.
[3] Chemist, Delta Fertilizers Company in Talkha, Egypt
[*]E-mail: asfouda@hotmail.com

The expired pantoprazole sodium EPS drug was studied as a corrosion inhibitor for high carbon steel (HCS) in 1 M HCl solution using mass loss (ML), potentiodynamic polarization (PP), electrochemical impedance spectroscopy (EIS) and electrochemical frequency modulation (EFM) tests. Fourier transform infrared spectroscopy (FT-IR) was utilized to identify bands of PS drug on HCS surface. Surface morphology was tested by scanning electron microscope (SEM), Atomic Force Microscopy (AFM) and Energy Dispersion Spectroscopy X-ray spectra (EDX). The effect of temperature on the corrosion process has been studied in addition of different concentrations of EPS drug. PP curves showed that the study drug is a mixed kind inhibitor. The inhibition efficiency (IP %) was improved with improving the concentration of PS and was reduced by improving the temperature of the medium. The PS adsorbed on HCS surface was noticed to follow the Langmuir's adsorption isotherm. The outcome data gotten from electrochemical and chemical tests are in excellent agreement.

Keywords: Corrosion inhibition, HCl, HCS, EPS drug, AFM, FT-IR, SEM

1. INTRODUCTION

Acid solutions are utilized for the elimination of unwanted measure and corrosion product in numerous manufacturing routes [1]. HCl and H_2SO_4 are extensively utilized in the pickling procedures of metals. The inhibitors utilized are one of the best ways for the defense in contradiction of corrosion in solutions with acid to preclude reduction of metal [2, 3]. The utilized of organic compounds containing hetero atoms, for example nitrogen, sulfur, and oxygen were used to decrease the steel corrosion [4–7]. The presence of π- electrons and lone pairs in molecules of inhibitor enable electron movement from an inhibitor to the outward of metal, creating a covalent bond. The toxic materials were utilized as inhibitors have been imperfect due to they're environmental threat. Consequently,

materials inclosing non-toxic and natural inhibitors have utilized as inhibitors [8–13]. In the recent years, drugs have used as corrosion hindrance. The drugs have used as corrosion hindrance for metals and alloys has some benefits over the use of organic/inorganic inhibitors due to their environmental surroundings [14]. Drugs are non-hazardous, low-cost, insignificant negative influence on the environment, so it's recommended substituting the traditional toxic corrosion hindrance [15]. Examination efforts have been prepared recently on utilize of antibacterial drugs as corrosion hindrance for metals in different media [17]. Gece [18] evaluation from literature utilizes of many kinds of drugs as corrosion hindrance of numerous metals. Ampiclox, ampicillin, cloxacillin, methocarbamol, tetracycline, penicillin G, azithromycin, orphenadrine etc, have been creating to be excellent corrosion hindrance for metals [19]. Flucloxacillin, amoxicillin has examined as corrosion hindrance for Al [20]. Cefalexin, cefadroxil, and cefazolin are utilizing as inhibitors for iron corrosion in acidic medium [21].

The choice of this drug EPS as a corrosion inhibitor is based on the resulting: i) EPS molecule comprises oxygen, nitrogen and sulfur atoms as active centers ii) this drug is apparently environmentally friendly and significant in biological reactions [22] and iii) PS drug can easily produce and disinfected [23]. EPS tested as a corrosion hindrance for HSC in acidic medium by different techniques and showed high IP %.
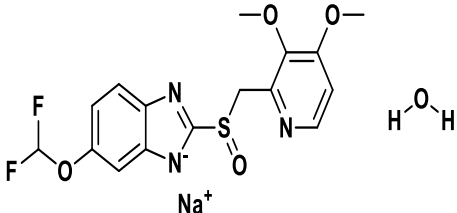
2. EXPERIMENTAL TESTS

2.1. The composition of HCS samples

HCS is an alloy with a composition of 0.55 – 0.93 % C, 0.3- 0.9 % Mn and the rest iron

2.2. Solutions

The corrosive solution utilized was ready by dissolving of analytical reagent grade, 37% HCl with bi-distilled water. The normal solution (1000 ppm) of EPS was utilized to prepare the wanted doses by dilution with bi-distilled water. The concentration of EPS utilized was 100-300 ppm. The structure of EPS is shown below:

Structure	Crystal structure	Mol. Formula & Mol. Weight
	6-(Difluoromethoxy)-2-[[(3,4-dimethoxy-2-pyridinyl)methyl]sulfinyl]-1H-benzimidazole sodium salt hydrate **(Pantoprazole Sodium Sesquihydrate)**	$C_{16}H_{16}N_3NaO_5S$ 423.07

2.3 Mass loss (ML) tests

Seven HCS coins of area $20 \times 20 \times 2$ mm were polished by successive emery papers till 2000 grit size, cleaned with bi-distilled water and acetone. All the corrosive acid solutions were exposed to air. The IP % and the surface coverage, θ, of EPS were computed from Eq. (1):

$$\% \text{ IP} = \theta \times 100 = [1- (CR_{inh}/ CR_{free})] \times 100 \qquad (1)$$

Where CR_{free} and CR_{inh} are the corrosion rate without and with EPS, respectively.

2.4 Electrochemical methods

All tests were conducted by utilizing a three-electrode glass cell involving of the HCS coins as (WE) working electrode ($1cm^2$), saturated calomel electrode (SCE) as a reference electrode and platinum gauze as the auxiliary electrode. These tests have carried out on HCS electrode in 1.0 M HCl solution with and without different concentrations of EPS at 25^oC and at constant conditions. All the electrochemical tests have conducted employing Gamry apparatus PCI300/4 Potentiostat/ Galvanostat/Zra analyzer**.**

2.4.1 Potentiodynamic polarization (PP) method

PP diagrams were given by exchanging the potential of an electrode from -600 to +400 mV vs SCE with a scan fraction of 1 mVs^{-1}. Stern-Geary test was, utilized for the determination of (i_{corr}) and (E_{corr}) were determined by extrapolating both Tafel lines to a point which given (log i_{corr}) and (E_{corr}) for inhibitor free acid and in presence of EPS. Then i_{corr} was utilized to compute the %IP and (θ) as follows:

$$\%IP = 100 \times \theta = 100 \times [1-(i_{corr}/i^{\circ}_{corr})] \qquad (2)$$

Where $i_{corr(inh)}$ and $i_{corr(free)}$ are current obtained from corrosion with and without of EPS drug, respectively.

2.4.2 EIS method

EIS tests were conducted in frequency medium (100×10^3 Hz to 0.1 Hz). All EIS values were close-fitting to a suitable equivalent circuit utilizing the Gamry Echem software Analyst. From the analysis of Nyquist plots, one can calculate R_{ct} and C_{dl}. The % IP and θ were measured from the EIS tests using Eq. (3):

$$\%IP = 100 \times \theta = [1-(R_{ct}/R_{ct}^{\circ}{}_{corr})] \times 100 \qquad (3)$$

Where R^o_{ct} and R_{ct} are the resistances without and with EPS drug, respectively.

2.4.3 EFM method

EFM results were achieved by relating potential perturbation sign with amplitude 10 mV with two sine waves of 2 and 5 Hz. The high peaks were utilized to calculate EFM parameters.

2.5 SEM Studies

Surface features (20 x 20 x 4 mm) of HCS were tested after dipping the coins in solutions containing and not containing 300 ppm EPS drug for one day. JEOL JSM-5500 was utilized for this analysis. These specimens were used for all surface analysis.

2.6 FT-IR analysis

The formation of complexes on HCS surface was observed by FT-IR spectroscopy reading utilizing IR (Perkin-Elmer) spectrophotometer at the central Lab, Faculty of Pharmacy, Mansoura University, Egypt which was utilized for plotting the FT-IR   HCS and EPS drug.

2.7 Atomic force microscope (AFM) analysis

Surface analysis of the HCS was studied utilize AFM (Park systems, XE-100 model). Contact mode was used with a scanner proportion of 0.8 Hz and the scan area was 5 μm x 5 μm. After liquefaction in 1.0 M HCl solution with and without 300 ppm of EPS drug for one day at 25^0C.

2.8 Energy dispersive X-ray (EDX) tests

The EDX tests were utilized to calculate the presence of element on the apparent HCS surface after one-day immersion in HCl and with 300 ppm drug.

3. RESULTS AND DISCUSSION

3.1 Mass loss (ML) tests

ML was carried out for HCS in 1 M HCl and with different concentration of EPS and is given in Fig. 2. % IP data measured are recorded in Tables 1 and 2, it is distinguished that the % IP rise with raising the EPS concentration and decreases with increasing the temperature from 30-50°C

Table 1. The corrosion rate ($k_{corr.}$), θ and %IP given from mass loss method for HCS in 1 M HCl with and without different concentrations of EPS at 30°C and 120 min immersion

Conc., ppm	ML, mg cm^{-2}	$k_{corr.}$, x10^{-4} mg cm^{-2} min^{-1}	Θ	% IP
Blank	4.729	39	---	---
100	0.674	5.6	0.857	85.7
150	0.533	4.4	0.887	88.7
200	0.488	4.1	0.897	89.7
250	0.399	3.3	0.916	91.6
300	0.316	2.6	0.933	93.3
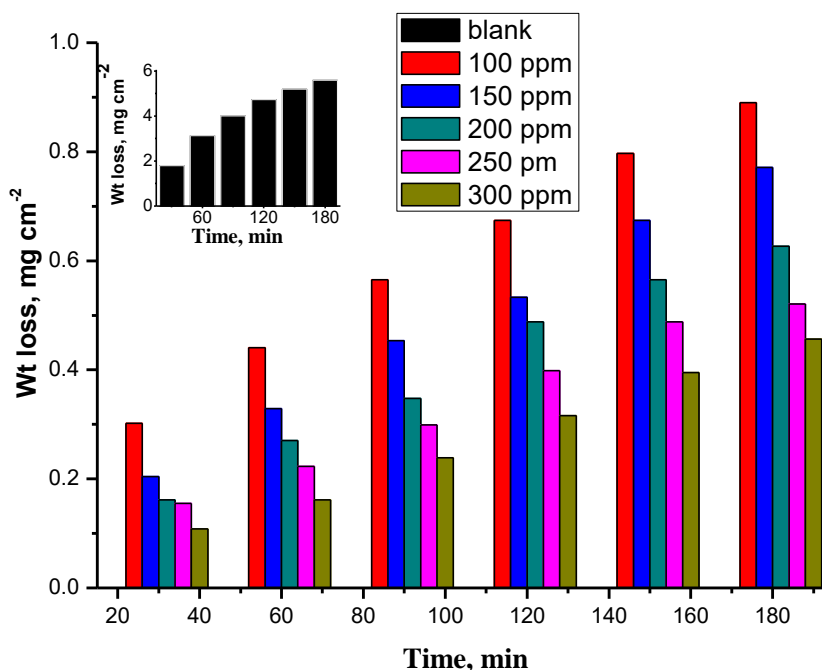
Figure 1. ML-time diagrams for the HCS corrosion in 1 M HCl and in presence of various EPS concentrations at 30°C

The molecules of EPS are adsorbed on HCS surface. The formed layer of the adsorbed drug molecules isolates the apparent surface of HCS from the HCl medium which limited the dissolution of HCS from corrosion. By increasing the concentration of EPS, k_{corr} decreased and %IP increased [24] as shown in Table 2.

3.2 Kinetic-thermodynamic parameters

The energy of activation (E^*_a) for corrosion of the HCS has calculated from the slope of log k_{corr} versus 1/T of plots by utilizing Arrhenius eq. (5) (Fig.2):

$$k_{corr} = A \exp(-E_a^* / RT) \tag{5}$$

Where E^*_a is the activation energy, R is a universal constant gas, and A is Arrhenius pre-exponential element. E_a^* increases in the presence of the EPS drug (Table 3). This increase in E^*_a indicates the rise of the thickness of the barrier layer formed on HCS surface. Therefore, by raising the temperature, % IP of EPS will decrease due to the increase of the number of molecules desorbed from the HCS surface. This result proposes that EPS control the corrosion by raising E^*_a. This happened by adsorption EPS on the surface of HCS which build an energy barrier for charge transfer. So the greater data of E^*_a in presence of EPS drug propose that the adsorption of EPS on HCS surface is physical.

Table 2. Effect of temperature on k_{corr}, θ, and %IP of HCS with and without different concentrations of EPS.

Conc., ppm	Temp., °C	k_{corr}, x10^{-4} mg cm^{-2}min^{-1}	θ	% IP
100	30	3.3	0.857	85.7
	35	4.0	0.841	84.1
	35	5.6	0.823	82.3
	45	7.0	0.763	76.3
	50	7.6	0.722	72.2
150	30	3.0	0.887	88.7
	35	3.6	0.868	86.8
	35	4.4	0.842	84.2
	45	6.0	0.788	78.8
	50	6.3	0.762	76.2
200	30	2.6	0.897	89.7
	35	3.0	0.891	89.1
	35	4.1	0.861	86.1
	45	5.2	0.823	82.3
	50	5.4	0.795	79.5
250	30	2.2	0.916	91.6
	35	2.3	0.899	89.9
	35	3.3	0.881	88.1
	45	4.4	0.863	86.3
	50	4.8	0.823	82.3
300	30	1.7	0.933	93.3
	35	1.8	0.919	91.9
	35	2.6	0.909	90.9
	45	3.7	0.894	89.4
	50	3.9	0.854	85.4
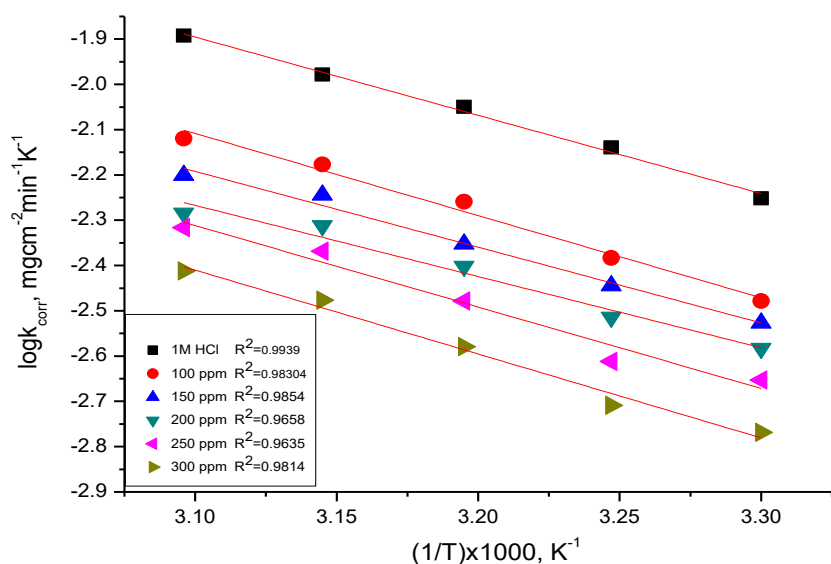
Figure 2. Log k_{corr} – 1/T curves for HCS without and with different concentrations of EPS drug

From the relation between 1/T vs log (k_{corr}/T) obtained in (Fig. 3), we can calculate the change of (ΔS^*) and (ΔH^*) from Eq. (6). The measured data are recorded in (Table 3)

$$k_{corr} = (RT/ N h) \, e^{(-\Delta H^*/RT)} \, e^{(\Delta S^*/R)} \qquad\qquad (6)$$

h is constant Planck's, and N is the Avogadro's number. The negative sign of ΔS^* for the EPS drug pointed that activated complex in the of transition rate determining step prefers an association rather than a dissociation step, so the decreasing in disorder occurred throughout the sequence from reactant to the started complex [27]. The ΔH^* has a negative sign indicate that the corrosion process is an exothermic process.
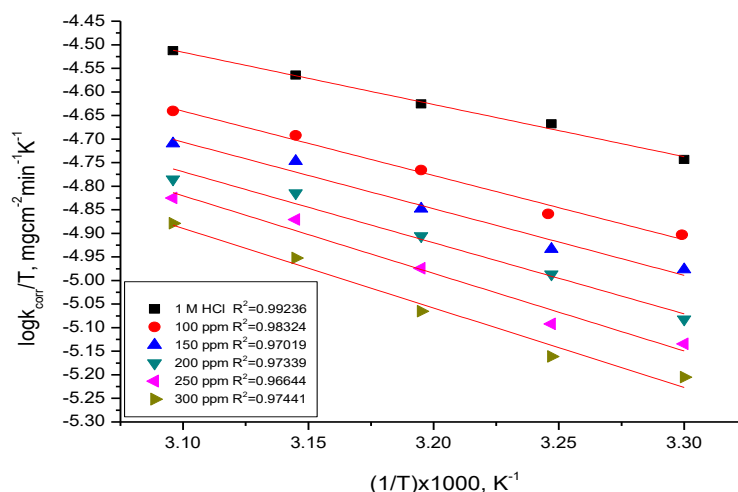
Figure 3. Log k_{corr} /T – 1/T diagrams for HCS in with and without of different concentrations of EPS drug

Table 3. Activation parameters for HCS corrosion with and without different concentrations of EPS drug

| Conc. ppm	E_a^*, kJ mol^{-1}	- ΔH^*, kJ mol^{-1}	-ΔS^*, J mol^{-1}K^{-1}
Blank	25.7	9.2	218.3
100	32.9	11.3	205.5
150	35.8	11.7	203.9
200	36.1	12.5	199.5
250	38.5	13.6	192.2
300	47.3	14.0	191.0

3.3 Adsorption isotherms

It's used to identify the type and degree of interaction among surface of metal and molecule of inhibitor. The organic molecule adsorbed due to the energy for interaction among an inhibitor and a metal is greater than between molecules of water and metal [25]. To gain the adsorption isotherms, (θ) given to ML test was obtained at different concentrations of EPS. The θ data were then used to fit the

most appropriate model of adsorption. From the results, it was found that the best (θ) fitted by Langmuir adsorption isotherm as in Fig. 4 [26]:
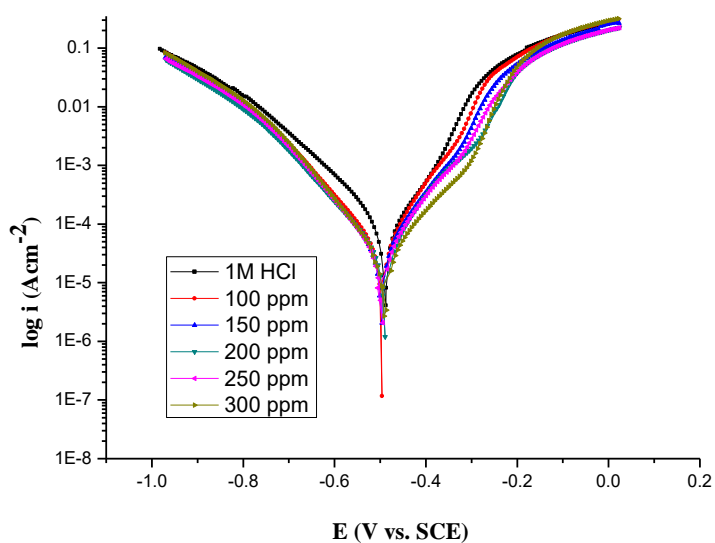
$$C/\theta = 1/K + C \tag{4}$$

Where C is concentrations of EPS drug, K_{ads} is the adsorption equilibrium constant
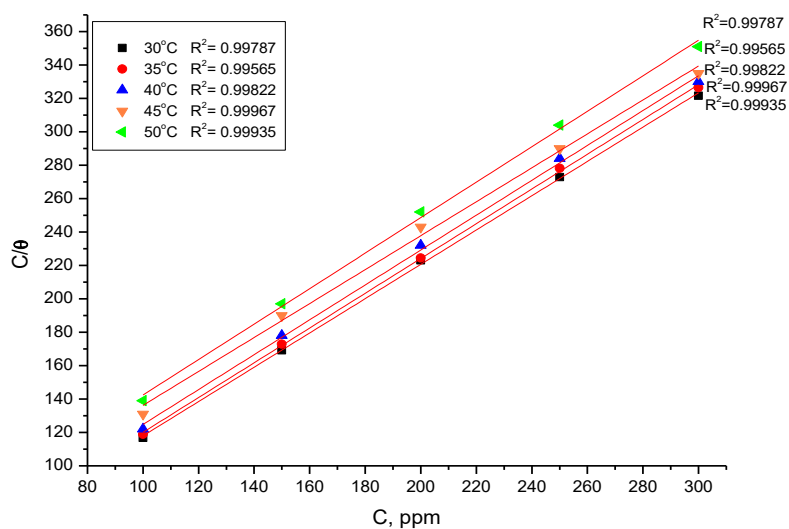
Figure 4. Langmuir curves for HCS in 1 M HCl and in attendance of different concentrations of EPS at different temperatures

3.4. Potentiodynamic polarization (PP) methods

Figure 5. Potentiodynamic polarization plots for the HCS corrosion with and without different concentrations of EPS drug at 25˚C

Figure 5 shows PP diagrams for HCS without and with different concentrations of the EPS drug at 25ºC. With an increment of the concentration of EPS the i_{corr} values decreased, which lead to decreasing in the CR. The PP curves recorded the parameters in Table 4 as the dissimilarity of the data of (log i_{corr}) with the corrosion potential (E_{corr}), Tafel slopes (β_a, β_c), (CR), (θ) and (%IP). This means that both cathodic and anodic reactions of HCS electrode are changed slightly by EPS drug in acidic medium. The anodic and cathodic slopes were lightly varied with the improving the concentrations of EPS drug. This shows that EPS drug represents as a mixed-type inhibitor [28].

Table 4. Parameters measured utilizing Potentiodynamic polarization tests for the corrosion of HCS without and with different concentrations of the EPS drug at 25ºC

Conc., ppm	i_{corr}, $\mu A\ cm^{-2}$	$-E_{corr}$, mV vs SCE	β_a, mVdec^{-1}	β_c, mVdec^{-1}	k_{corr} mm y^{-1}	θ	%IP
HCl	169.0	489	246	193	77.31	--	--
100	20.6	496	51	68	9.42	0.878	87.8
150	17.7	491	57	75	8.08	0.895	89.5
200	13.6	491	46	59	6.21	0.920	92.0
250	10.3	490	48	54	4.70	0.939	93.9
300	8.3	497	41	46	3.77	0.951	95.1

3.5. EIS tests
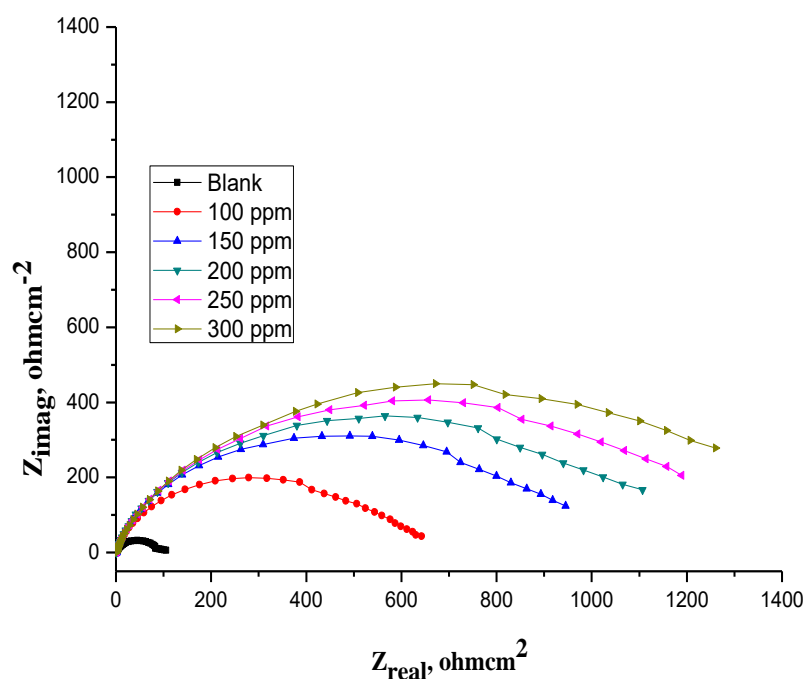
Figure 6. Nyquist diagrams obtained for HCS corrosion with and without different concentrations of EPS at 25ºC

EIS is confirming goodly test in research about corrosion [29]. Fig. 6 shows the Nyquist plots, given at OCP both with and without different concentrations of EPS at 25°C. The increase of the diameters of the capacitive loop with the adding of EPS drug was due to the rise in the thickness of the adsorbed layer formed on the HCS surface. Fig. 7, represents the Bode diagram with and without different concentrations of EPS drug (log f vs. log Z).
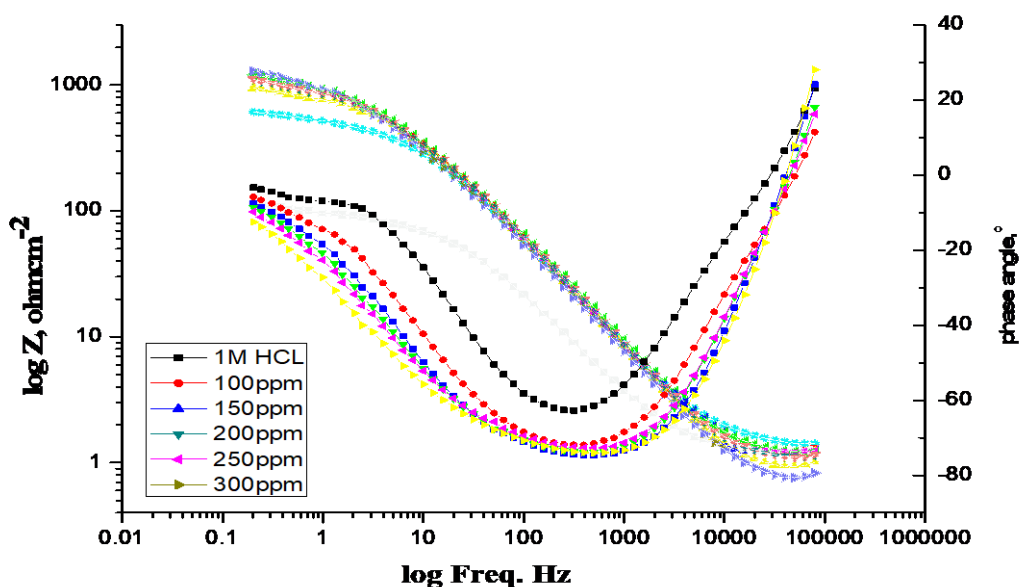

Figure 7. Bode diagrams obtained for HSC corrosion with and without different concentrations of the EPS drug at 25˚C

EIS data for EPS drug were measured utilizing the best equivalent circuit in Fig. 8, which signifies a distinct charge transfer and fits well with the obtained data. The CPE is put in the circuit in its place of a pure double layer capacitor to yield a maximum precise fit [30]. C_{dl}, was determined using eqs (7) and (8):

$$C_{dl} = Y_0 (\omega_{max})^{n-1} \tag{7}$$

$$\omega_{max} = 2\pi f_{max} \tag{8}$$

Where $Y_0 = $ the CPE degree and f_{max} is the frequency at which the imaginary constituent of the EIS is greatest. The obtained curves are very similar for all samples with and without different concentrations of EPS drug showing that no exchange in the corrosion mechanism [31]. Table 5 shows the impedance data which confirmed the data of R_{ct} rise with improving the concentration of the EPS drug and this pointed to the increase in % IP. This may be due to the increase of the thickness of the adsorbed layer by increasing the drug concentrations.
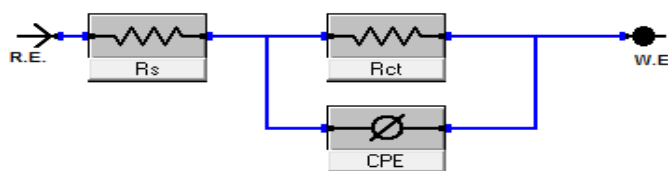
Figure 8. Electrical circuit utilized to fit the EIS values

Table 5. Impedance parameters for HCS in 1.0 M HCl solution with and without different concentrations of EPS at 25˚C

Conc., ppm.	R_{ct}, Ω cm^2	C_{dl}, x10^{-6}, μF cm^{-2}	θ	% IP
1 M HCl	89.15	84.1	---	---
100	564.80	50.9	0.842	84.2
150	828.80	45.4	0.892	89.2
200	969.30	43.5	0.908	90.8
250	1082.00	41.6	0.918	91.8
300	1143.00	37.2	0.922	92.2

The lower in CPE/C_{dl} data due to a lesser in local dielectric constant, signifying that EPS hindrance the HCS corrosion by metal/acid adsorbed [32, 33].

3.6. Electrochemical frequency modulation (EFM) test

Table 6. Electrochemical parameters obtained from EFM tests for HCS with and without different concentrations of the EPS drug at 25°C

[inh], ppm	i_{corr}, μ A Cm^{-2}	CR mpy	CF-2	CF-3	θ	% IP
Blank	539	246	1.6	2.5	--	--
100	91	42	1.9	2.3	0.830	83.0
150	85	38	1.8	3.1	0.840	84.0
200	75	34	1.5	2.6	0.860	86.0
250	73	33	1.5	3.3	0.865	86.5
300	58	26	1.9	2.7	0.892	89.2

EFM is a nondestructive corrosion analyses test [34]. The EFM diagrams for HCS in the presence and absence of (100 – 300 ppm) EPS were recorded and shown in Fig. 9 by raising the EPS concentration, i_{corr} has reduced to a lower value. Table 6 showed that the EPS has recorded the displacement of corrosion potential lower than 85 mV in different concentrations of the uninhibited solution. So, the EPS drug sets as a mixed kind inhibitor. The largest peak has utilized to calculate (i_{corr}), the Tafel slopes (β_c and β_a) and causality factors (CF-2 and CF-3). Table 6 displays the electrochemical parameters which characterize that the EPS drug impede the corrosion of HCS in HCl

among adsorption. %IP rise by improving the examine drug concentrations and was measured as eq (2).
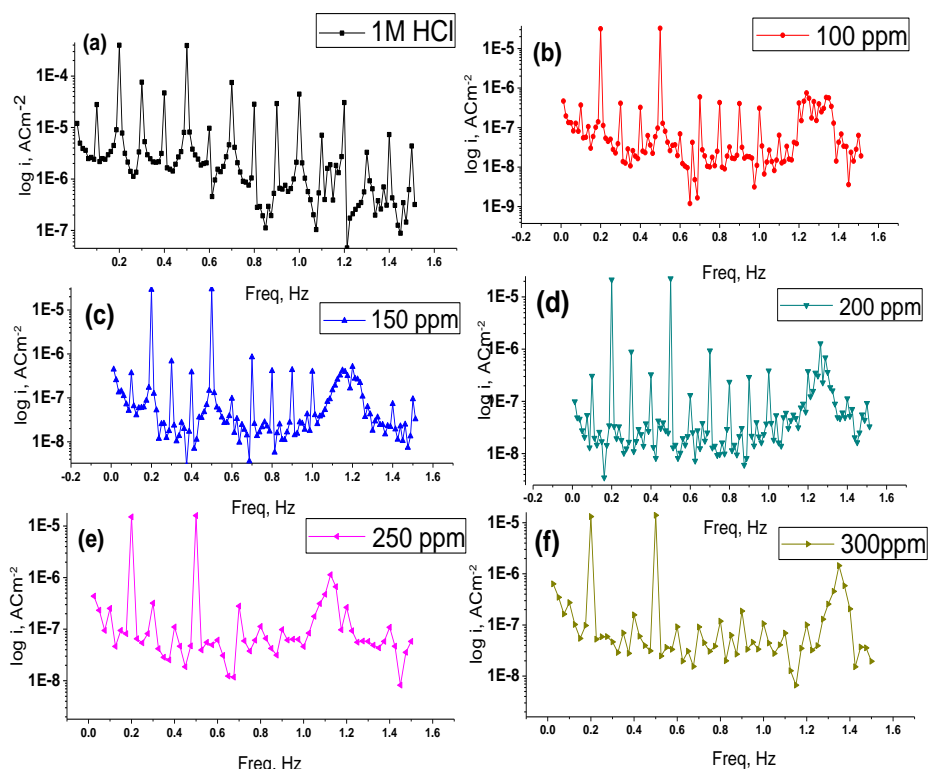
Figure 9 (a-g). EFM data for the corrosion of HCS in with and without different concentrations of EPS at 25°C

3.7 Fourier transform infrared spectroscopy *(FTIR) Analysis*

The FTIR spectrum method based on analyzing the protective film found on the HCS surface [35] Fig.(10a) shows the FTIR spectrum of the pure EPS The -C–F stretching frequency of the alkyl halide group performs at 1280 cm^{-1} with a strong band. The – O–C stretching frequency seems as three strong bands at 1019, 1041 and 1078 cm^{-1}which indicating three ether bonds in pure EPS. The – OH stretching frequency of the alcohol group appears at 3281 cm^{-1}which has strong and broad intensity [36]. The –CN stretching frequency performs at 1205 cm^{-1}. The –C=C– stretching frequency appears as multiple bands between (1400-1600) cm^{-1} which indicating the multiple double bonds in the in pure EPS drug. The data in Fig (10b) showed that – C –F extending frequency has moved from 1280 cm^{-1} to 1313 cm^{-1}. The– O –C extending frequency has moved to make from three bands to one weak band at 1068 cm^{-1}. The – OH extending frequency has moved from 3281 to 3420 cm^{-1}.The –CN extending frequency has moved from 1205 cm^{-1} to 1230 cm^{-1}. This statement recommends that P.S has coordinated with Fe^{2+}, among the atomic oxygen of the carboxyl assembly and atom nitrogen of the amine assembly, given the formation of the Fe^{2+}- EPS complex at the anodic sites of the HCS surface [37].
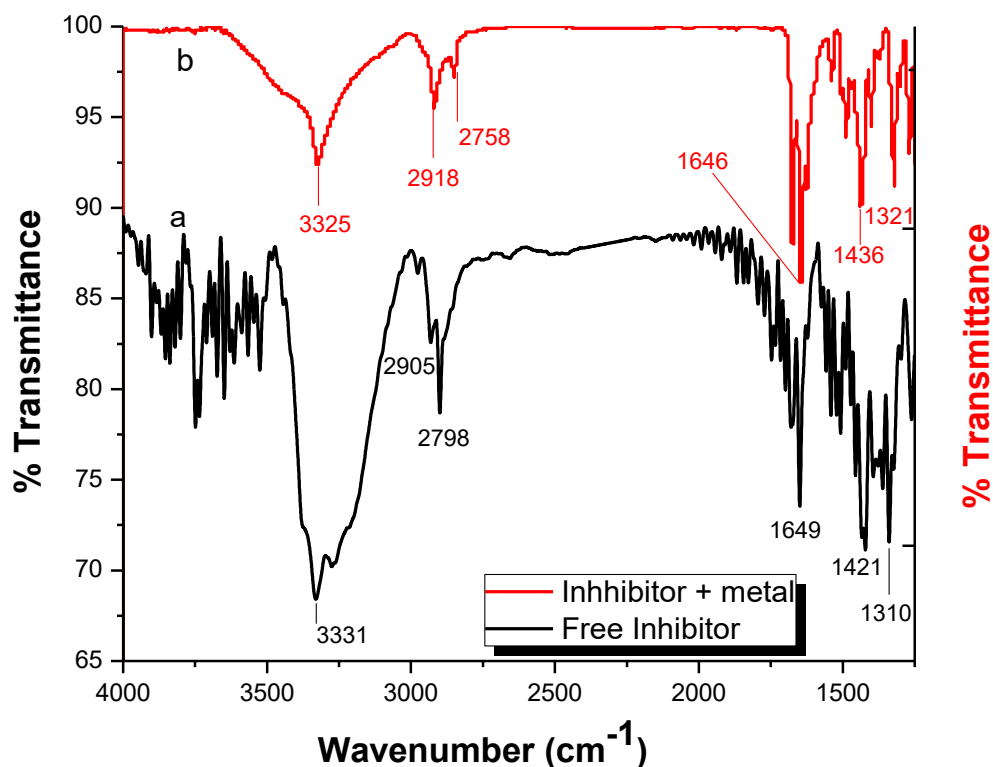
Figure 10a.b FTIR of pure EPS and FTIR of film found on the HCS surface after immersing in a
solution containing EPS

3.8 SEM test
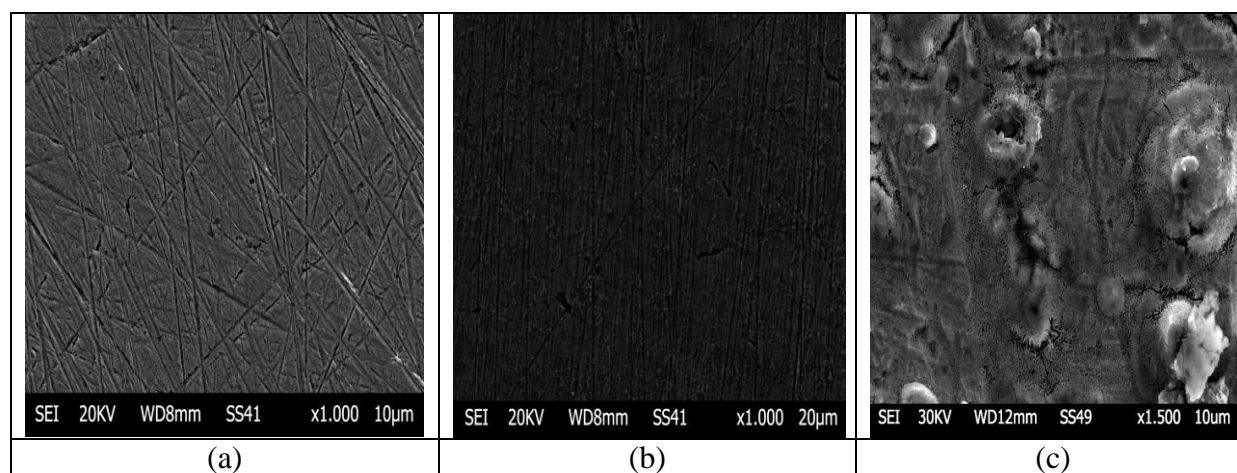
Figure 11. SEM image of HCS surface (a) previously of immersing in 1 M HCl, (b) afterward 24
hours of immersing in 1 M HCl and (c) afterward 24 hours of immersing in 1 M HCl + 300
ppm of EPS at 25°C

To investigate the metal surface changes after immersion in acidic solution with and without
EPS drug. The HCS surface was analyzing using SEM. The HCS samples in 1 M HCl solution with
and without of the highest concentration of the EPS (300 ppm) for one day have exposed to analysis.

Fig (11) shows SEM micrographs. It is clear that HCS surface corrosion has reduced by the presence of the EPS drug. The other pictures revealed that there is high damage, several pits and cavities on the HCS surface in the absence of EPS drug more than the presence of it. This shows that metal surface was covered with adsorbed protective molecules of EPS [38].

3.9 Energy dispersion spectroscopy (EDX) studies

| (a) EDX test on HCS (free) HCS in1M HCl | (b) Blank | (c) HCS immersing in acid with the presence of EPS |
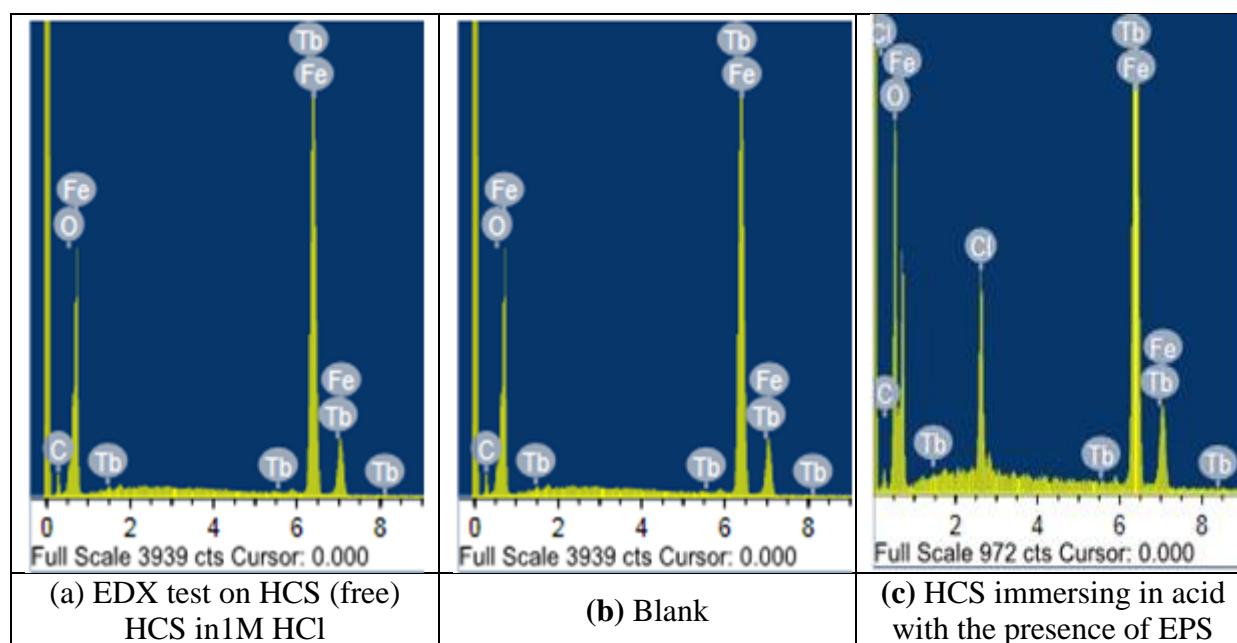
Figure 12. EDX analysis on HCS (free) (b) Blank of HCS in1M HCl (c) HCS immersing in 1 M HCl with EPS for 24 hours immersion

Figure (12.a) gives the EDX of HCS only without the drug. The EDX test designates that only O and Fe were detecting, which displays that the inactive film enclosed only Fe_2O_3. Fig (12.b). Portray of the EDX test of HCS in acid only, Fig. (12.c) shows the EDX test of HCS in acid + 300 ppm of EPS drug. These data show that the C and N materials protected the HCS surface.

Table 7. Surface conformation (weight %) of HCS after 12h immersing in HCl with and without 300 ppm EPS drug

(Mass %)	Fe	Cl	C	O	Tb
HCS	87.51	--	9.19	3.05	9.26
Blank	81.22	--	8.35	--	10.43
P.S	59.99	5.42	5.42	23.91	5.26

*3.10 Atomic force microscopy (AFM) characterization*

AFM test supplies photos with atomic or near-atomic-resolution surface topography, which able to get the surface roughness of coins in the angstrom- scale [39]. Fig.(13. a) shows the three dimensional (3D) AFM morphologies for polished HCS surface as standard sample, Fig.(13. b) HCS surface inundation in 1M HCl as blank sample and Fig.(13. c) HCS surface inundation in 1M HCl +300 ppm of EPS [40]. AFM images were obtained to measure the mean roughness (Sa), the average root mean (Sq) and the peak height (Sp) for the polished HCS (free sample), HCS surface dipped in 1 M HCl (blank sample) and HCS surface dipped in 1M HCl + 300 ppm of EPS drug . The gotten data from AFM examine were recorded in Table 8.

Table 8. AFM data for HCS surface with and without of 300 ppm EPS drug

Sample	Sa	Sq	Sp
Free	20.63	24.79	60.26
Blank	694.90	810.95	1830.20
EPS drug	70.27	88.83	359.04
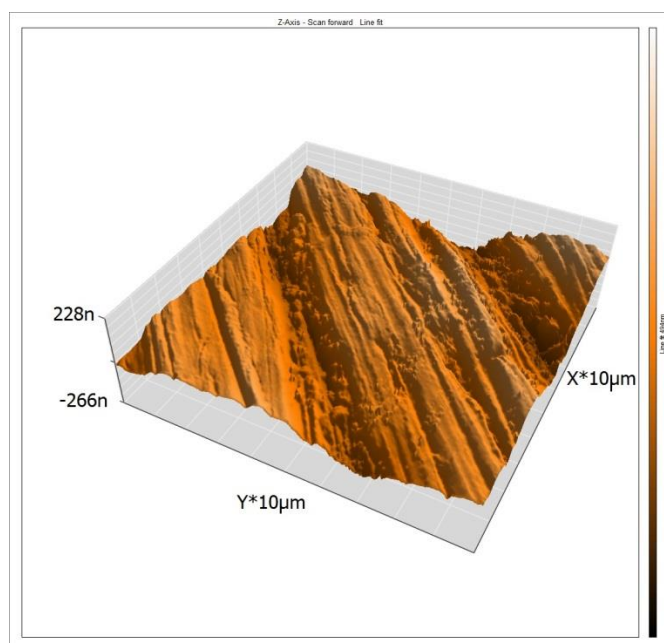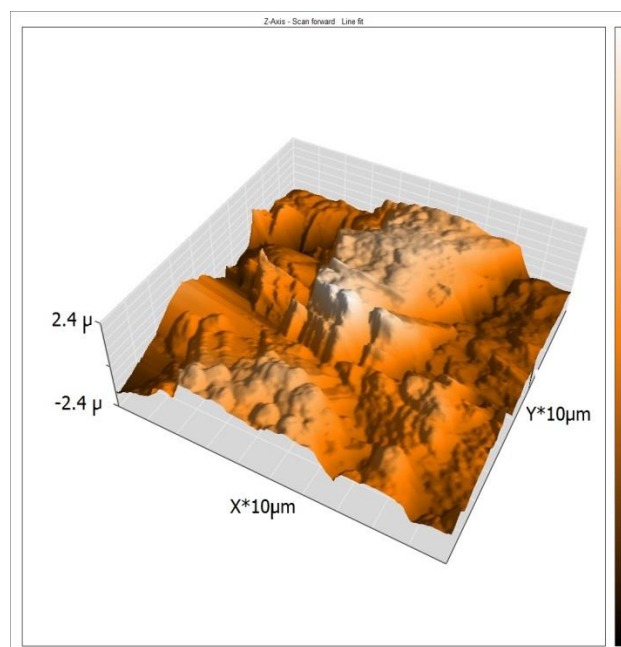
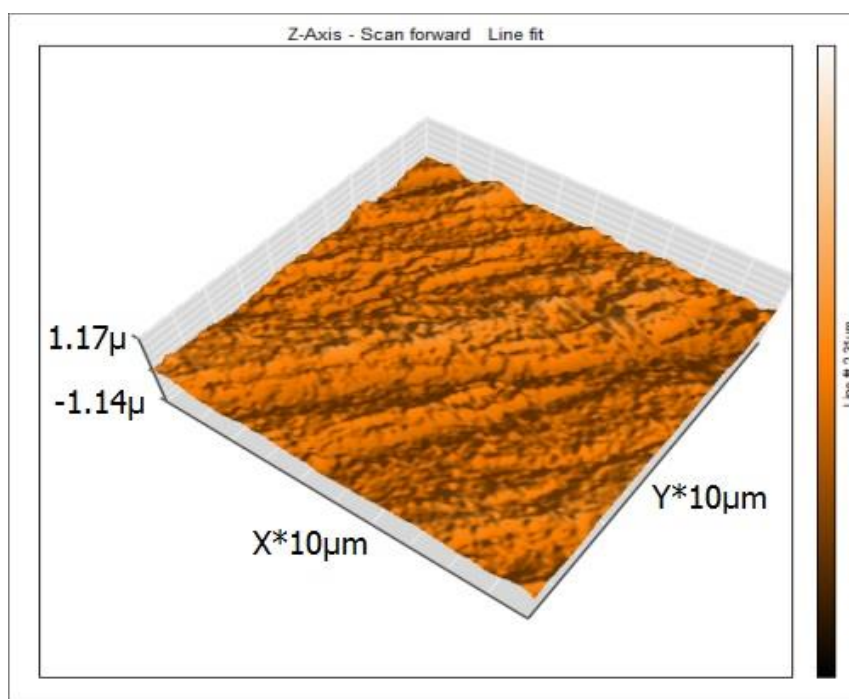**(a) Free**   **(b) Blank**
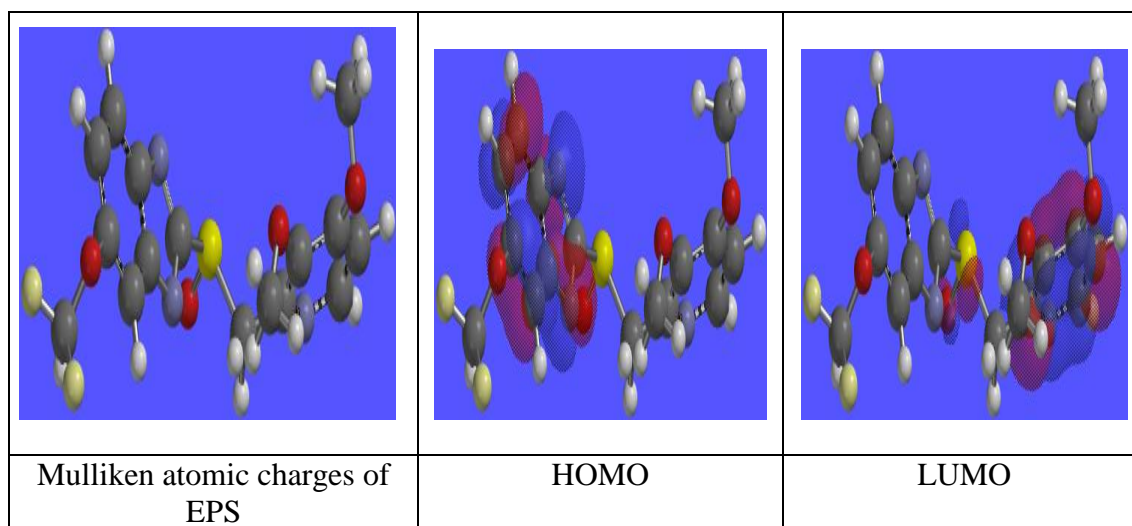
(c) Inhibitor

Figure 13. AFM 3D images of HCS: free (a) in 1 M HCl (b) and with 300 ppm EPS drug (c) after immersion for 24 hrs in the corresponding solution

3.11 Theoretical calculations

| Mulliken atomic charges of EPS | HOMO | LUMO |

Figure 14. Optimized orbital and Mullikan atomic of EPS drug

Some quantum chemical calculations can obtain to investigate the effect of drug structure of the EPS drug to study the efficiency of inhibition mechanism. Bond lengths and bond angles can optimize to give electronic structure and the geometry of the EPS inhibitor Fig (14) shows the optimized molecular structures of the EPS. The data gained from the quantum chemical parameter for investigating EPS as: Highest occupied molecular orbital (E_{HOMO}) = -4.8 eV, Lowest unoccupied

molecular orbital (E_{LUMO}) = 1.76 eV, Energy gap (ΔE) = E_{LUMO}- E_{HOMO} = 6.56 eV, Dipole moment (μ) = 12.53 Debye

E_{HOMO} is related to the electron donating aptitude of the molecule. The great data of E_{HOMO} are

Pointed to a penchant for the molecule to donate electrons to be suitable for the acceptor molecules which having small energy and vacant molecular orbitals. Thus (E_{LOMO}) pointed to the aptitude of the molecule to receive electrons. The lesser the data of E_{LUMO}, is more appreciated to the molecule accept electron [41]. The PI was improved with the lower negative E_{HOMO} energies and with decreasing the value of ΔE (energy gap) [42] and the stronger interaction among EPS and HCS surface. So, the interactions are more likely adsorbed physical. Fig (15. b) shows high data of the HOMO density were found in the vicinity of sulfur and nitrogen atoms, pointing to the nucleophilic center is the sulfur and nitrogen atoms.

3.12. Comparison of inhibition efficiency of some drugs for HCS in acidic solution

The % IE of the expired investigated drug for HCS in 1 M HCl solution and some of the previously reported drugs are recorded in Table 9. As can be seen in this Table the %IP of the present expired drug is comparable to or better than those of previously reported drugs at the same condition

3.13 Mechanism of corrosion inhibition

The prevention of corrosion of EPS drug on HCS in 1 M HCl solution based on the temperature, chemical structure and concentrations of it. By increasing the concentration of EPS drug, one found some changes as; a decrease of ML, an increase of (θ) and R_{ct} , a decrease of i_{corr}, and C_{dl} and rise of %IP. The mechanism of the protection processes of some groups of organic assemblies is due to their adsorption on the HCS surfaces and blocking the cathodic or anodic reactions or both. The adsorption process of EPS on the HCS surface has influenced by some factors as molecular size, the presence of active centers on the chemical structure of inhibitor, charge density and capabilities form complexes. The presence of heteroatoms in the chemical structure of EPS is responsible for the adsorption process and the formation of coordinate bonds through the transfer of lone pairs of electron of heteroatoms to the Fe surface, these species can adsorb on the metal surface [43]. Moreover, EPS may adsorb via the electrostatic interactions among protonated form of the EPS and the negatively charged HCS surface. On the other hand, EPS drug (Fig. 18) has characterized by the presence of chelation centers relating O and N atoms with lone pairs of electrons. Therefore, the formation of complexes of EPS and Fe^{2+} released during the corrosion reaction has considered possible. UV-Vis absorption spectra were shown, in order to approve the probability of establishment of the EPS-Fe complex. This analysis confirmed the formation of six-membered ring complexes with the Fe atoms on HCS surfaces, this complex adsorbed on HCS surface and isolates the metal surface from the corrosive solution.

Compound (1)
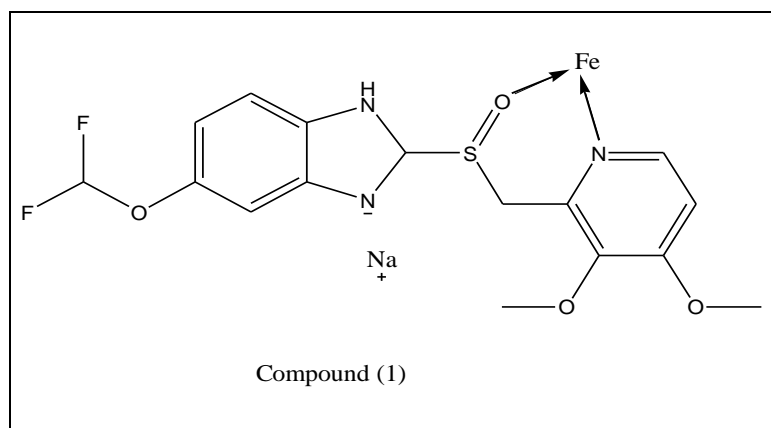
Table 9. Some drugs examined as corrosion inhibitors by other authors for HCS in 1M HCl and expired drug in this study

Inhibitor (drug)	Sample	Medium	IE %	References
Penicillin G (15×10^{-4}M)	MS	H_2SO_4	90.0	[44]
Penicillin V (15×10^{-4}M)	MS	H_2SO_4	63.3	[45]
Cefalexin (11×10^{-4}M)	MS	HCl	67.5	[46]
Ceftriaxone (400 ppm)	MS	HCl	87,6	[47]
Cefotaxime (300 ppm)	MS	HCl	90.0	[48]
Cefixime (8.8×10^{-4}M)	MS	HCl	62.0	[49]
Norfloxacin (50 ppm)	MS	HCl	22.3	[50]
Ciprofloxacin (50 ppm)	MS	HCl	20.8	[50]
Pefloxacin (50 ppm)	MS	HCl	15.1	[50]
Amifloxacin (50 ppm)	MS	HCl	17.1	[50]
Enofloxacin (50 ppm)	MS	HCl	18.3	[50]
Methocarbamol (2×10^{-3} M)	MS	HCl	67.1	[51]

4. CONCLUSIONS

Inhibitions of corrosion of the EPS drug towards the dissolution of HCS in 1M HCl solution via adsorption have confirmed. The % IP increased with improving the concentrations of EPS and with lowering temperature. The %IP of EPS drug is due to the formation of the insoluble adsorbed complex on the HCS surface and the process of adsorption obeyed Langmuir isotherm. The results obtained from EIS tests were parallel with PP test. SEM and AFM test also prove the formation of protecting film on the HCS surface in 1M HCl solution. The outcome data gotten from all tests and quantum chemical calculations were in excellent agreement.

References

1. A.S. Fouda, T. Fayed, M.A. Elmorsi, M. Elsayed, *J. Bio Tribo-Corros.*, 3(2017)33
2. A.S. Fouda, M. Abdallah, M. Yousef, *Chem. Sci. Rev. Lett.*, 3(11S)(2014)130
3. O.Benali, H.Benmehdi, O. Hasnaoui, C. Selles, R. Salghi, *J. Mater. Environ. Sci.*, 4(1) (2013)127

4. M.O.Zcan, R.Solmaz, G. Kardas, I.Dehri, *Colloids Surf.*, 325 (2008)57
5. L. Wang, *Corros. Sci.*, 48 (2006)608
6. K.Kermannezhad, A.N. Chermahini, M.M.Momeni, B.Rezaei, *Int. J. Chem. Eng. Appl.*, 306 (2016)849
7. S.Ramesh, S.Rajeswari, *Electrochim. Acta*, 49 (2004)811
8. A.S. Fouda, A.SW.Abousalem, G.Y.EL-Ewady, *Int J. Ind. Chem.*, 8 (2017)61
9. A.S.Fouda, G.Y.El-Ewady, A.H.Ali, *Green Chem. Lett. Rev.*, 10(2) (2017)88
10. A.S.Fouda, M.A.Elmorsi, B.S.Abou-Elmagd, *Polish. J. Chem. Technol.*, 19(1) (2017)95
11. E. Khamis, E.El-Rafey, A.M. Abdel Gaber, A.Hefnawy, N.G. Shams El-Din, M.S Esmail, *Desalination,* 57 (2016)235
12. M. El-Azzouzi, A. Aouniti, S. Tighadouin, H. Elmsellem, S. Radi, B. Hammouti, A. El Assyry, F. Bentiss, A. Zarrouk, *J. Mol. Liq.,* 221 (2016)633
13. J. H. Al-Fahemia, M. Abdallaha, A. M. Geadc,B. A. Jahdaly , *J. Mol. Liq.* 222(2016)1157
14. N.O. Eddy, S.A. Odoemelam, *J. Mater. Sci.*, 4 (2008) 87.
15. A.S. Mahdi, *Int. J. Adv. Res. Eng. Technol.*, 5(2014) 99
16. E.E. Ebenso, N.O. Eddy, A.O. Odiongenyi, *Port. Electrochim. Acta*, 27(2009)13.
17. A.K. Singh, S.K. Singh, E.E Ebenso, *Int. J. Electrochem. Sci.*, 6(2011)5689.
18. G. Gece, *Corros. Sci.*, 53(2011)3873**.**
19. A.S, Fouda, A. Abdallah, M. Yousef, *Chem. Sci. Rev. lett.*, 3 (2014)130.
20. M. Abdallah, *Corros. Sci.*, 46(2004)1981.
21. S.K. Shukla, M.A. Quraishi, *Mater. Chem. Phys.*, 120(2010)142.
22. N.O. Eddy, E.E. Ebenso, *Int. J. Electrochem. Sci.*, 5(2010)731.
23. S.A.Sahara, M.A.E.Sugimoto, T.A.Uotani, H.A.Ichikawa, M.A.Yamade, T.A.Kagami, Y.B.Hama D igestion, Phys. Rev., 91(2015)4.
24. V. Branzoi, F. Golgovici, F. Branzoi, *Mater. Chem. Phys.*, 78 (2002)122.
25. M. M. Saleh, A. A. Atia, *J. Appl. Electrochem.*, 36 (2006) 899.
26. X. H. Li, S. D. Deng, H. Fu, *Corros. Sci.*, 51(2009) 1344
27. V. R. Saliyan, A.V. Adhikari, *Bull. Mater. Sci.*, 31 (2007) 699.
28. Z. H. Tao, S. T. Zhang, W. H. Li, B.R.Hou, *Corros. Sci.*, 51 (2009)2588.
29. M. El Achouri, S. Kertit, H .M. Gouttaya, B. Nciri, Y. Bensouda, L. Perez, M. R. Infante, K. Elkacemi„ *Prog. Org. Coat.*, 43(2001) 267.
30. S. F. Mertens, C. Xhoffer, B. C. Decooman, E. Temmerman, *Corrosion*, 53(1997) 381.
31. A. J. Trowsdate, B. Noble, S. J. Haris, I. S. R. Gibbins, G. E. Thomson, G. C. Wood, *Corros. Sci.*, 38 (1996) 177.
32. F. M.Reis, H. G. De Melo, I. Costa, *J. Electrochem. Acta*, 51 (2006)1780.
33. H. Ma, S. Chen, L. Niu, S. Zhao, S. Li, D. Li, *J. Appl. Electrochem.*, 32 (2002) 65
34. E. Kus, F. Mansfeld, *Corros. Sci.,* 48 (2006) 965.
35. H. Amar, T. Braisaz, D. Villemin, *Mater Chem Phys.*, 110 (2008)1.
36. R. Kalaivani, B. Narayanasamy, J. A. Selvi, *Port. Electrochim. Acta*, 27 (2009)177.
37. J. Sathiyabama, S. Rajendran, A. A. Selv, *Open Corrosion J.*, 2 (2009)77.
38. I. You, P. Zhao, Q.Liang, B. Hou, *Appl. Surf. Sci.,* 252 (2005)1245.
39. R. Nagalakshmi, L. Nagarajan, R. J. Rathish, S.S. Prabha, N. Vijaya, J. Jeyasundari and S. Rajendran, *J. Nano Corros. Sci. Eng.*, 1 (1) (2014) 39.
40. R. Vera, R. Schrebler, P. Cury, R. Del Rio and H. Romero, *J. Appl. Elecrochem.*, 37 (2007) 519.
41. I. Lukovits, K. Palfi and E. Kalman, *Corrosion*, 53 (1997) 915.
42. A. Popova, M. Christov, S. Raicheva and E. Sokolova, *Corros. Sci.,*46 (2004)1333.
43. O. A.Hazazi1, M. Abdallah, *J. Electrochem. Sci.*, 8 (2013) 8138.
44. N. O. Eddy, S. A. Odoemelam, P. Ekwumemgbo, *Sci. Res. Essays*, 4 (2009) 33.
45. N. O. Eddy, S. A. Odoemelam, *Adv. Nat. Appl. Sci.*, 2(2008) 225.
46. A. K. Singh, M. A. Quraishi., *Corros. Sci.*, 52 (2010) 152.

47. S. K. Shukla, M. A. Quraishi*, J. Appl. Electrochem*., 39(2009) 1517.
48. S. K. Shukla, M. A. Quraishi, *Corros. Sci*., 51(2009) 1007.
49. I. Naqvi, A. R. Saleemi, S.Naveed, *Int. J. Electrochem. Sci*., 6(2011)146.
50. S. Acharya, S. N. Upadhyay, *Trans. Indian Inst. Met.,* 57 (2004)297.
51. E. E. Ebenso, N. O. Eddy, A. O. Odiongenyi, *Port. Electrochim. Acta*, 27 (2009)13.